Application of Phase Detection Frequency Domain Reflectometry for Locating Faults in an F-18 Flight Control Harness

You Chung Chung, *Senior Member, IEEE*, Cynthia Furse, *Senior Member, IEEE*, and Jeremy Pruitt, *Member, IEEE*

***Abstract*—The performance of a phase-detection frequency-domain reflectometer (PD-FDR) for locating open and short circuits (hard faults) in a Navy F-18 flight control harness has been tested, and the analytical expressions for accuracy verified. Nine different types of aircraft wires appear in this harness: twisted pair, shielded wires with 1–4 inner conductors, "filter wire," and bundles of individual wires. PD-FDRs in a variety of frequency ranges (12–25, 100–220, 150–300, and 180–400 MHz) are compared. Signal processing techniques are utilized to remove the reflections where the PD-FDR is connected to the wire harness, which is critical to obtaining accurate measurements, particularly for short lengths of wire. For this specific application, open and short circuits are located to within 2.5 cm (1 in) for PD-FDR200 and 11 cm (5.5 in) for PD-FDR25 for wires ranging from 9 cm to 9.15 m (6–360 in).**

***Index Terms*—Aging wire, frequency domain reflectometer (FDR), wire fault location, reflectometry.**

I. Introduction

AGING wiring in aircraft, trains, cars, and other transportation equipment, nuclear power plants, buildings, commercial products, and large machinery has been identified as an area of critical national concern [1]–[3]. As the average age of both military and commercial airline fleets moves well into their teen years, this problem has received extensive national attention, and several methods for testing wires have been developed [1].

One of the major classes of wire fault location methods is reflectometry, where a low voltage signal is sent down the wire, and reflections that occur from the end of the wire or other anomalies along its length are detected at the transmitting end. These systems can be divided into three broad classes—time domain, spread spectrum, and frequency domain reflectometry, depending on the shape of the signal that is sent down the wire.

Time domain reflectometry (TDR) [4], [5] launches a short rectangular step of voltage down the cable (shaped pulses can also be used), and the wave travels to the far end of the cable, where it is reflected back and analyzed at the source end. The time delay between the incident and reflected voltages indicates the length of the cable, and its magnitude and polarity indicate the impedance at the discontinuity. TDR has also been identified as a potential method for locating small anomalies such as frays or chafes if an extremely accurate initial baseline is available [6]–[8].

Spread spectrum reflectometry [9]–[11] sends a psendo-noise (PN) code down the wire and correlates the returned reflection to determine the fault location. The digital PN code appears as random noise to the existing signal, therefore enabling the system to run live and potentially in flight.

Frequency domain reflectometry (FDR) [also called swept frequency reflectometry (SFR)] sends a set of stepped-frequency sine waves down the wire. These waves travel to the end of the cable and are reflected back to the source, where either the reflected waves or the standing wave produced by the superposition of the incident and reflected waves are analyzed. There are three types of frequency domain reflectometry that are commonly used in radar applications and can also be adapted for measurement of wires and cables. These are frequency-modulated continuous-wave (FMCW) systems [12], Standing wave reflectometry (SWR) systems [13], [14], and phase-detection frequency-domain reflectometry (PD-FDR) systems [15]–[17], [19], [20]. While these systems are very well understood for radar applications, their use on lossy, noncontrolled impedance wires that are not impedance matched to the test systems has not been previously addressed in the literature. Since these considerations require special filtering algorithms and strongly impact how the test frequency range and computational requirements control the system accuracy, these are important to address. This paper describes the test results, design tradeoffs, and a method to improve resolution (particularly for short lengths of wires) for PD-FDRs applied to a realistic F-18 harness. This harness includes a wide variety of common aircraft wire types, and the results that are seen are typical of what is observed for other aircraft wiring systems. A filtering algorithm to remove the effect of the nonideal connection between the PD-FDR and the wire is demonstrated to improve the accuracy and enable measurement of short lengths of wire. Many of these considerations must also be applied to other reflectometry methods.

Section II describes the F-18 flight control harness including the types of wires and their characteristics and layout. Section III describes the operation of the PD-FDR. Section IV gives detailed results that demonstrate the PD-FDR design tradeoffs and

Manuscript received August 1, 2003; revised April 21, 2004. This work was supported in part by the Federal Laboratory Consortium (FLC) under a Small Business Innovative Research (SBIR) contract modification to NAVAIR under Contract N68335-98-C-0036 for Management Sciences Inc.

Y. C. Chung is with the Information and Communication Engineering Department, Dae Gu University, Kyungsan, Kyungbuk 712-714, Korea (e-mail: youchung@daegu.ac.kr).

C. Furse is with the Department of Electrical and Computer Engineering, University of Utah, Salt Lake City, UT 84112 USA and also with the LiveWire Test Laboratories Inc., West Valley City, UT 84120 USA (e-mail: cfurse@ece.utah.edu).

J. Pruitt is with the Signal Exploitation and Geolocation Division, Southwest Research Institute, San Antonio, TX 78238 USA.

Digital Object Identifier 10.1109/TEMC.2005.847403

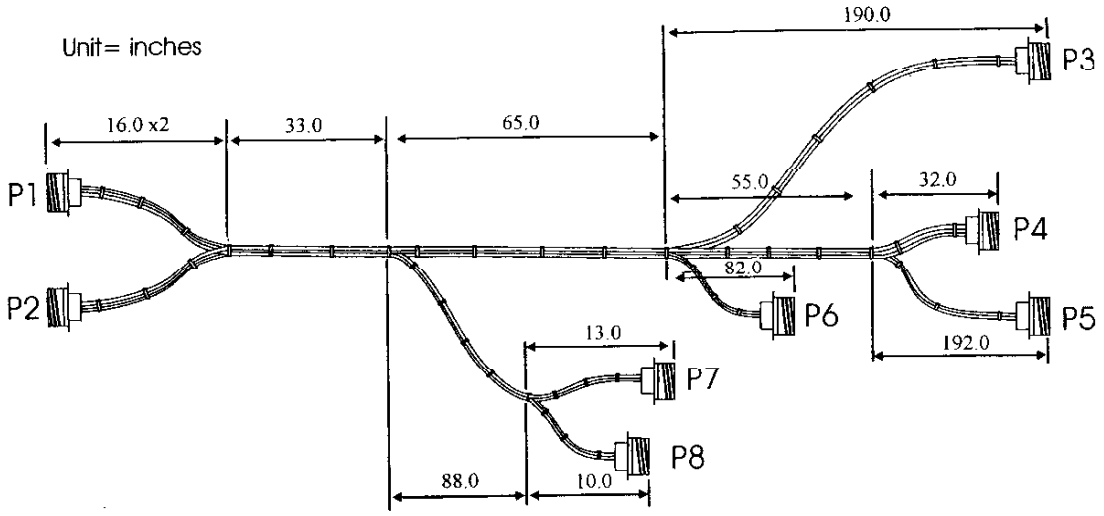

Fig. 1. F-18 flight control harness mock up and system diagram.

TABLE I
LENGTH, VELOCITY OF PROPAGATION, AND IMPEDANCE OF F-18 CABLES. ($C = 3 \times 10^8$ m/s)

Wire #	Wire Part Number	Wire description	Length in inches	Measured Velocity of Propagation	Impedance in ohms
2	M85485-12-24U2A	Filter Line, Black shielded twisted pair	304	0.26C	92~100
3	M27500-24SE2S23	shielded twisted pair	201	0.66C	60
4	M27500-22SR2G23	shielded twisted pair	150	0.67C	42
5	M27500-24SC3S23	shielded triple	304, 147	0.66C	52
6	M27500-22SP1S23	coax (single inner conductor, shielded)	201, 196, 150	NA	25
7	M27500-24SC2U00	Twisted pair wires	196	0.71C	120
8	M22759-43-26-9	Single (AWG 26)	361	0.76C	120~250
9	M27500-22SC4S23	shielded quadruple	361	0.69C	54
10	M22759-43-22-9	Single (AWG 22)	196, 150	0.71C	140~200

verify the design equations for realistic aircraft wires. As seen in the conclusion, Section V, the PD-FDR is an effective method of locating hard faults (open or short circuits) to within 2.5–11 cm (depending on wire type) for the F-18 flight control harness. Partial open or short circuits cannot be detected, as they do not produce sufficient reflection for detection. This method is demonstrated for unpowered harnesses. Similar results would be expected for other wiring harnesses.

II. F-18 Aircraft Cable Harness and Cables

An F-18 aircraft flight control harness was mocked up specifically for these tests, using the wire types, connectors, layout, and wire tie locations that are typical for that aircraft, as shown in Fig. 1. It was built on an aluminum board, with the wires attached by stick-on holders and cable ties to represent a typical distance between the harness (which is not shielded) and the body of the aircraft. The harness consists of eight D38999/20WG35SN wall mount plug connectors (P1–P8) where each connector terminates in 79 female pins. All of the wires are bundled and tied at about 3-in intervals, and tied to the board with plastic wire ties every 6 in.

There are nine different wire types in the harness. The lengths of the wires range from 150 to 362 in long, and the types of wires are listed in Table I. The nine different types of the wires can be divided into four different groups of specifications: single (ie. not shielded, and not twisted with another wire. These single wires are "paired" with another single wire running parallel for testing), shielded (1–4 conductors), twisted pair (but unshielded) and filter line cable (which deliberately attenuates high frequency signals). The single wire has the center multi-strand conductors insulated by the plastic material. The twisted pair wire consists of two twisted single wires. The shielded wire has multiple twisted single wires inside of the metal shield and the outer plastic insulation. The filter line cable is specially insulated twisted pair deliberately designed to attenuate high frequencies (above 50 MHz).

The wires have been tested with a time domain reflectometer (TDR) [18] to measure impedance and velocity of propagation. The velocity of propagation is shown in Table I, and the impedance is shown in Figs. 2 and 3. The impedance is relatively constant along the length of the shielded wires (controlled impedance cables), but is somewhat erratic (varying by perhaps 10%) for the unshielded wires (noncontrolled impedance cables).

The loss on the wires was measured with a source and spectrum analyzer, and these normalized losses for 10 in of wire are plotted in Fig. 4. The filter line (M85485-12-24U) and the thin

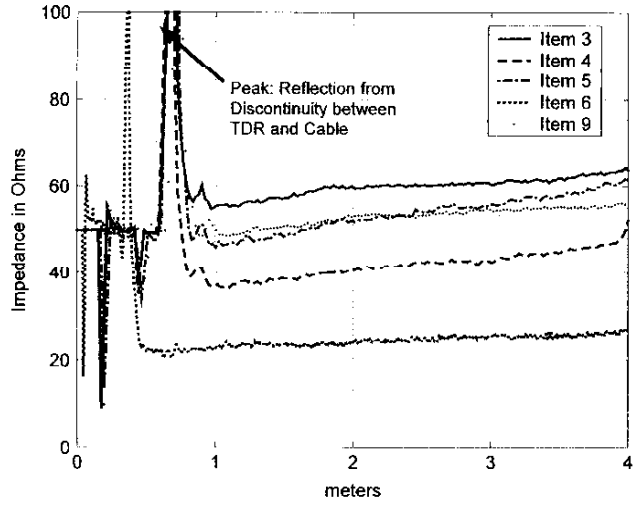

Fig. 2. Impedance of the shielded F-18 cables.

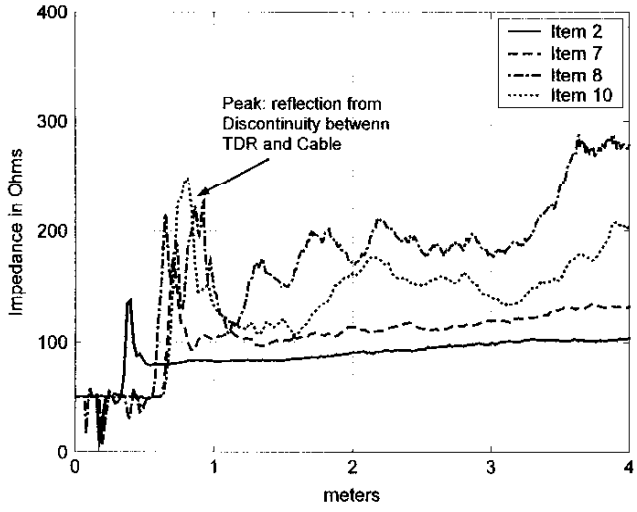

Fig. 3. Impedance of the filter line and unshielded F-18 cables.

single wire (M22759-43-26) are the most lossy cables. When a cable has 1 dBm loss per 10 in, the loss of the return signal for reflectometry measurements will be 20 dBm for 100 in of cable, since the signal makes a round trip to the end back, thus doubling the loss. High frequency signals are heavily attenuated due to this loss, so the lowest possible practical frequency should be used. The tradeoff is that lower frequency PD-FDR units generally have less accuracy (because of smaller bandwidth available in lower frequency components) and a longer "dead zone" (minimum length of cable that can be measured using traditional methods). New signal processing techniques to improve the accuracy of lower frequency PD-FDR units is described in Section IV.

III. PD-FDR System Operation

A PD-FDR [15]–[17], [19] block diagram is shown in Fig. 5. The PD-FDR units reported in [19] have 10 dB more attenuation than those in this paper, as a different directional coupler was used. A voltage-controlled oscillator (VCO) provides

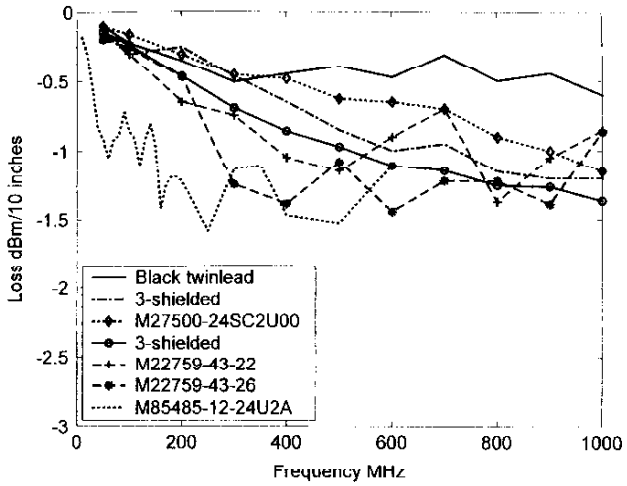

Fig. 4. Loss of cables (per 10 in of cable) in the F-18 harness versus frequency.

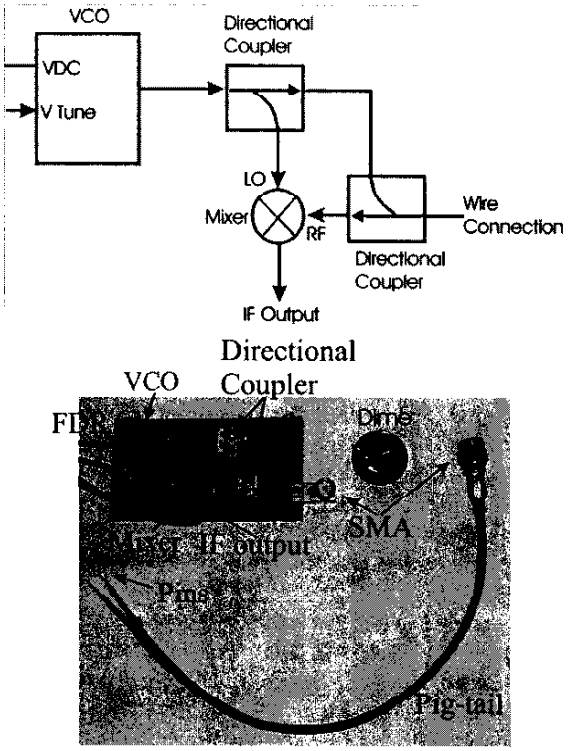

Fig. 5. Block diagram and photo of the PD-FDR with a pig-tail.

a sinusoidal signal that is stepped over a given bandwidth (f_1 through f_2) with a specific frequency step size Δf. An analog voltage from a digital to analog (D/A) converter from a microprocessor unit (mpu) controls the frequency, which is stepped up throughout the test. The VCO signal is split in the 10-dB directional coupler. Ten decibels of the incident power is sent to the mixer as a sample of the original sinusoid, and the remainder is sent to the cable. The incident signal travels down the cable and reflects back from the load (typically very high or very low impedance) at the end. The superposition (sum) of the reflected and the incident waves forms a standing wave on the cable. The reflected wave is isolated from the incident wave by the second

TABLE II
MAXIMUM LENGTH AND RESOLUTION OF PD-FDR OPERATING IN DIFFERENT FREQUENCY BANDS (V_p HAS BEEN SET TO 0.67 cm/s)

	Bandwidth in MHz	Frequency Step in MHz	**Maximum measureable Length (L_{max}) in meters**	Length of FFT	**Resolution of Length (ΔL) in meters**
PD-FDR1000	420-1040	2.4219	20.74 m	1024	0.0405
				2048	**0.0203**
PD-FDR400	200-400	0.78125	62.4 m	1024	0.125
				2048	**0.0628**
PD-FDR300	150-300	0.585938	85.76 m	1024	0.1675
				2048	**0.0837**
PD-FDR200	100-220	0.46875	104 m	1024	0.2093
				2048	**0.10468**
PD-FDR100	43-113	0.2734375	178 m	1024	0.35893
				2048	**0.17946**
PD-FDR25	12-36	0.0488281	998 m	1024	2.01
				2048	**1.005**

directional coupler and is sent to the mixer. The mixer "multiplies" the frequency on the radar frequency (RF) port by the frequency on the intermediate frequency (IF) port. The mixer output has three frequency components—the RF frequency, an upper sideband frequency at RF + IF, and a lower sideband at RF − IF. When RF and IF are at the same frequencies as they are in PD-FDR, this lower sideband is at zero frequency (dc). This dc voltage at the mixer output is the signal that we will detect and use to determine the length and load of the line. An analog-to-digital (A/D) converter effectively acts as a low-pass filter and removes the higher frequency components, because it does not have sampling speeds to accommodate them.

The number of cycles in the dc mixer output as it is stepped through the frequency range is proportional to the distance (L) being measured. The fast Fourier transform (FFT) of this waveform will give a Dirac delta function (single spike) at a location we will call *Peak*. Therefore, the location of *Peak* in the FFT response will be proportional to the length of the wire. The length is found from this peak index by

$$L = 2L_{\text{Max}}\left(\frac{\text{Peak} - \text{Peak}(0)}{N_{\text{FFt}} - 1}\right) = \frac{1}{2}\left(\frac{\text{Peak} - \text{Peak}(0)}{N_{\text{FFt}} \quad 1}\right)\left(\frac{N_F - 1}{f_2 - f_1}\right) v_p \tag{1}$$

where

Peak	location of the Dirac delta peak in the FFT (an integer value);
v_p	velocity of propagation in the cable (meters per second);
f_1	start frequency of the PD-FDR (Hertz);
f_2	stop frequency of the PD-FDR (Hertz);
N_F	number of frequencies in the PD−FDR = integer$[(f_2 - f_1)/\Delta f]$;
Δf	frequency step size for PD-FDR (Hertz);
Peak	peak index for corresponding length in FFT;
Peak(0)	peak index for 0 length;
N_{FFT}	number of points in the FFT (an integer value, generally 1024, 2048, 4096, or 8192).

This equation can be used for FFT lengths larger than measured data sets, by zero padding the measured data. This method improves the resolution of the results. The maximum length ($L_{\max}$) that can be measured is limited by the frequency step size

$$L_{\max} = \frac{v_p}{4\Delta f}. \tag{2}$$

The resolution (accuracy) of the measurements (ΔL) is given by

$$\Delta L = v_p/(2N_{\text{FFT}}\Delta f). \tag{3}$$

Note that longer FFTs give better accuracy. This becomes especially important when low frequency PD-FDR units (with smaller Δf due to hardware constraints) are used for lossy wires.

PD-FDR units with various frequency ranges were tested in this paper. They are: PD-FDR400: (200–400 MHz, Δf = 0.78 MHz), PD-FDR300: (150–300 MHz, Δf = 0.58 MHz) PD-FDR200: (100–220 MHz, Δf = 0.47 MHz), PD-FDR100: (43–113 MHz, Δf = 0.27 MHz) and PD-FDR25: (12.5–25 MHz, Δf = 0.049 MHz). Table II shows the comparison of maximum length and resolution of these PD-FDR units as a function of the length of the FFT.

IV. TEST RESULTS OF PD-FDRS AND METHODS TO REDUCE THE BLIND SPOTS ASSOCIATED WITH SHORT WIRES

The wires in Table I were tested using the method described in Section III. Fig. 5 shows how a "pig-tail" connects the SMA connector on the PD-FDR and the sockets in the wire connector. The harness could not be "sacrificed," so additional pieces of wire of the types and lengths listed in Table I were bundled with the harness and cut every 4–6 in.

Fig. 6 shows the dc mixer output as a function of frequency for the PD-FDR200 for triple shielded cables (Table I, item 5) of lengths 362 in (9.19 m), 230 in (5.84 m), and 82 in (2.08 m). Particularly for the wires that are 362 and 230 in long, there is a significant low frequency signal mixed with the expected high frequency signals. This low frequency component is from the "pig tail" used to connect the circuit to the wire under test (in our case, a 6-in 50-Ω coaxial line terminated in male pins). When the FFT is used to extract these frequencies from the

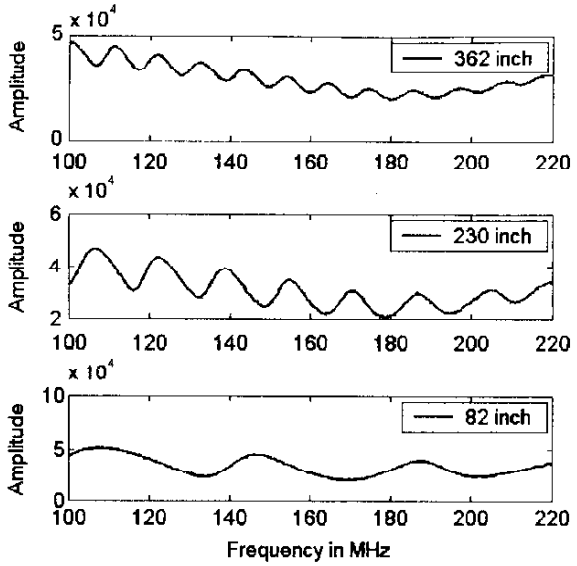

Fig. 6. Response of PD-FDR200 for shielded twisted triple cables (Table I, item 5).

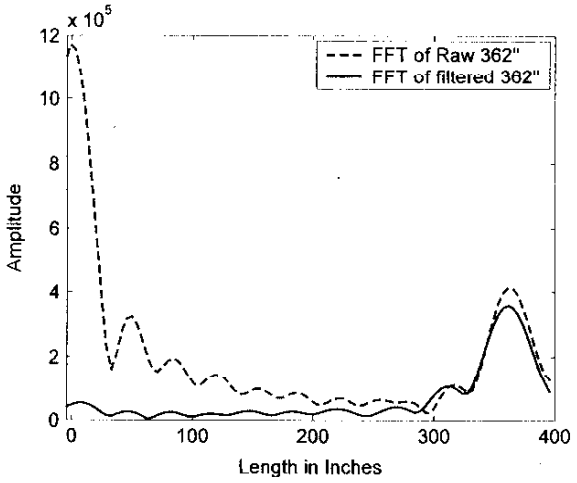

Fig. 7. FFT of filtered and nonfiltered 36-in-long shielded triple cable (Table I, item 5) with the PD-FDR200. Predicted length is 361.5 in with a 2048–point FFT).

data, a very high low frequency peak is observed, as shown as the dashed line in Fig. 7. This low frequency peak interferes with proper identification of the higher frequency peak associated with the wire length, and would completely obscure data from shorter lengths of cables that have lower frequency responses. This "blind spot" is seen in all reflectometry methods, when the wire is short enough that the incident and reflected signals overlap. This is a particular limitation for measuring aircraft wiring, as the majority of faults are seen within 2 ft of the connector, probably due to wear and tear during maintenance. Thus, a filtering process is needed to remove this unwanted low frequency information while retaining information on short wires.

There are many ways to filter out the low frequency component. A high pass filter could be used, but a typical high pass filter changes the original phase of the signal (and hence the

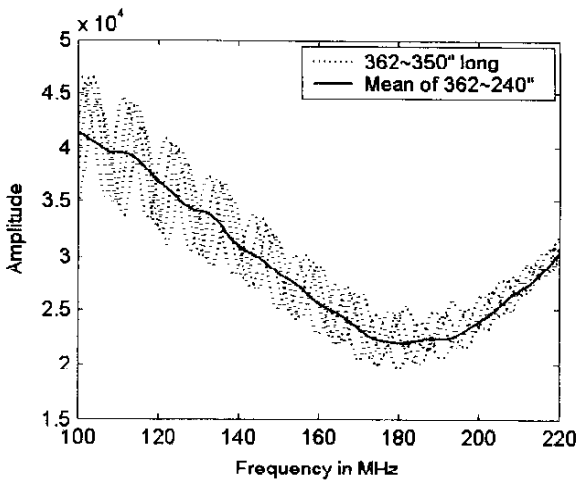

Fig. 8. Averaged low frequency noise signal (solid line) obtained by averaging the 30 raw data samples from wires 362 to 240 in long (in steps of 4 in) for shielded triple cable with PD-FDR200.

calculation of the type of open or short fault encountered). Perhaps even more problematic, the filtering process distorts the expected signal for short wires, giving huge errors in their analysis. The second filtering method is to predict the low frequency component, since it is the same for all cable lengths, and remove it from the measured signals. This can be done in the frequency domain (after the FFT of the data is taken), and was found to work for longer lengths of wires, but it still caused excessive errors for shorter lengths of wires. Much better results were found by predicting the low frequency component from the raw signal before the FFT processing. The prediction of the low frequency component is obtained by averaging the signal of several wires close to the maximum length of interest. Fig. 8 shows the signal of 362, 358, 354, and 350 in lengths with dashed lines, and the low frequency signal (solid line) obtained by averaging about 30 of the signals from 362 to 240 in long. After removing the low frequency component from the raw data, the 2048-point FFT of the signal for the 362-in-long cable has been plotted in Fig. 7 with the solid line. It shows only one peak, which corresponds to the correct length of the wire. The effectiveness of this filtering method for a wide range of cable lengths is shown in Fig. 9. Lengths of wires from 362 to 4 in are correctly identified by a single responding peak. Without this method, the 4- and 10-in wires could not be detected at all, and the measurements of the other wires were less accurate. In Fig. 10, the amplitude of the 10-in wire is lower than the amplitude of the 82-in wire. This is because the magnitude of the 10-in reflection is reduced more than that of the 82-in wire by the filtering. This does not have a significant impact on the length measurement, however it would have an impact on calculation of the magnitude of the load impedance. It should be noted that all of these filtering methods works better for longer cables than shorter cables, because the frequency from the cable is significantly separated from the frequency from the pigtail in that case, and can be filtered with less loss to the desired measurement signal.

So far we have described how the low frequency component from the pigtail can be removed. The relationship between the remaining peak locations and the length of the wires can be

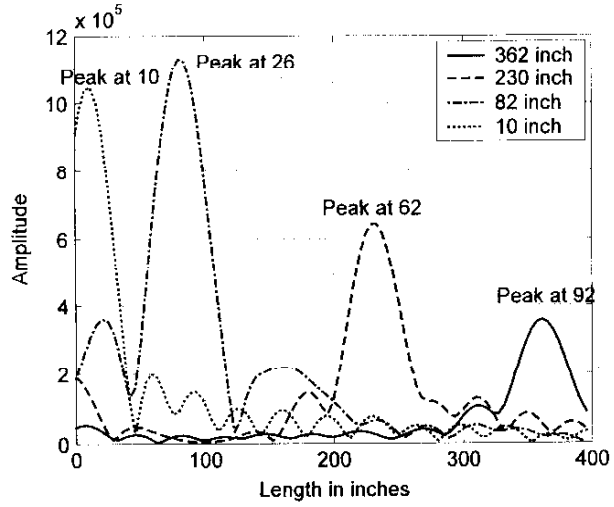

Fig. 9. Peak positions of 2048-point FFT versus length of the shielded triple wire with PD-FDR200.

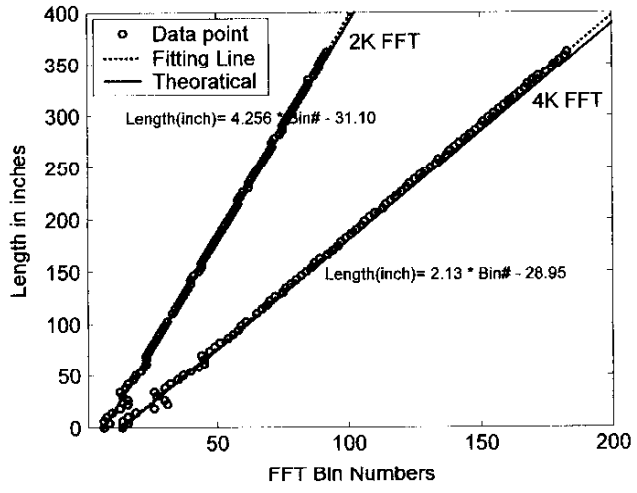

Fig. 10. Relationship between calculated length and measured peak location of 2048- and 4096-point FFTs for shielded triple wire measured with the PD-FDR200.

found two ways. The first uses (1) with a theoretical or measured velocity of propagation. This method does not account for any phase shifts within the electronics, and velocity of propagation measurements are not always readily available, so a slightly more accurate method is to simply measure the longest and shortest cables of interest for each type of wire, and use the line through those two points to calculate wire length. The methods give the same results to within about 2%. The linear equations for the F-18 harness for the PD-FDR200 (and PD-FR25 in cases where the line was too lossy for the PD-FDR200) are given in Table III for FFT lengths of 1024, 2048, 4096, and 8192. We have found the second method to be easier to apply. In practice, there is a finite (albeit large) set of aircraft wire types, which could be measured in the laboratory and entered into a database for later use during onboard measurements.

Note that each set of measurements includes only about 256 frequency steps, so the higher resolution FFTs are found by the traditional method of zero-padding the end of the array. Fig. 10 shows the measured data for the triple shielded wire, which was cut every 4 in to evaluate the accuracy of this method. The predicted resolution (ΔL) based on (3) is 4.2 in with 2048-point FFT. The observed accuracy is 8.7 in, 4.3 in, 2.2 in, and 1.0 in for 1024-, 2048-, 4096-, and 8192-point FFTs, respectively.

Use of lower frequency PD-FDR signals is necessary on very lossy lines. The PD-FDR25, for instance, is the only frequency range that we tested that was capable of measuring the filter wires. The ability to use low frequency hardware can have a significant cost savings, although it did not in our application, because we used hardware that was as similar as possible for all PD-FDR units. The disadvantage of the low frequency PD-FDR would be loss of resolution due to the smaller bandwidth available in these components, but this can be ameliorated by using larger FFT lengths by zero padding the data. The measured accuracies of the 1024-, 2048-, 4096-, and 8192-point FFTs are 18, 9.4, 4.7, and 2.3 in, respectively with the PD-FDR25, for wire type 2. Other wire types show similar improvement in accuracy with increased FFT length as shown in Table III.

An F-18 flight control harness was used to evaluate the accuracy and efficacy of a phase-detection frequency domain reflectometry method for locating cable faults. Seven types of wires including both controlled and noncontrolled impedance cables were included in the harness. PD-FDR units ranging from 25 to 400 MHz were evaluated. The loss on some types of wire (filter wire especially) prohibited the use of the higher frequency PD-FDR units. The observed accuracy for each wire type, PD-FDR frequency range, and length of the FFT is tabulated in Table III along with the expected accuracy for each case. The expected accuracy was met or exceeded in all cases, giving confidence in the design equations provided in this paper. The increase in accuracy (and associated increase in required computational power) for longer FFT calculations was verified, and an effective method of filtering out the inherent low frequency component from the data was demonstrated. These test results show that phase detection frequency domain reflectometry is, indeed, a viable method for locating hard faults on realistic aircraft cables and verifies the design tradeoffs necessary to obtain a desired accuracy. Fig. 11 shows the measurements for a shielded quadruple cable that is 361 in long for the PD-FDR in the 200-, 300-, and 400-MHz ranges using a 1024-point FFT. The filtering process has been done for all tests. Due to attenuation on the wire, the peak of the 400-MHz PD-FDR is too small to detect, and the responses of the 200-MHz PD-FDR and 300-MHz PD-FDR are shown as peak indexes 46 and 61, respectively. Although a small peak is observed, the response of the 300-MHz PD-FDR is also not strong enough to give reliable data, but the 200-MHz PD-FDR is usable for measurement.

Theoretically, the FDR response for open and short circuited cables should be 180° out of phase. In practice, there is a significant phase difference, but not exactly 180° as shown in Fig. 12(a) and (b) for a 214-in M27500-22SC4S23 shielded quadruple wire. The peak index using the 2048-point FFT for short circuited wires is identical to open circuited wires, as expected. Unfortunately, the phase of the open and short is not correctly predicted from the analytical results, due to nonlinear phase shifts within the hardware itself, and varies from wire to

TABLE III
SLOPE AND OFFSET OF LINEAR EQUATIONS OF WIRES WITH PD-FDR200 (FOR ALL TESTS EXCEPT WHEN NOTED AS PD-FDR25). (LENGTH OF WIRE = SLOPE * PEAK INDEX + OFFSET, ACCURACY = ±SLOPE)

Item number	Wire Part Number	Wire description	1024 FFT Slope, Offset	2048 FFT Slope, Offset	4096 FFT Slope, Offset	8192 FFT Slope, Offset
2	M85485-12-24U2A **PD-FDR25**	Filter Line, Black shielded twisted pair	18.122, -33.94	9.3769 -33.5372	4.6752 -28.0901	2.3468 -26.3396
3	M27500-24SE2S23	shielded twisted pair	8.3564 - 26.2319	4.2058 -22.8857	2.1036 -21.0836	1.0501 -19.7616
4	M27500-22SR2G23	shielded twisted pair	7.9906 -16.9990	4.0002 -10.8967	1.9947 -8.5337	0.9992 -7.8375
5	M27500-24SC3S23	shielded triple	8.6632, -38.093	4.267, -31.10	2.1306, -28.95	1.0647 -27.7155
6	M27500-22SP1S23	Coax (shielded single)	8.7701 -24.6882	4.3804 -19.9024	2.1962 -17.9987	1.0941 -16.4443
7	M27500-24SC2U00	Unshielded twisted pair	9.0958 -21.2417	4.5368 -16.6101	2.2596 -13.5691	1.1303 -12.6444
8	M22759-43-26-9 **PD-FDR25**	Thin single AWG 26 (paired with another single in the bundle)	40.8590 -8.4197	19.9763 22.2644	10.6300 16.0773	5.4247 15.8182
9	M27500-22SC4S23	shielded quadruple	8.2581 -17.3652	4.1385 -9.6184	2.0735 -8.0051	1.0362 -6.9525
10	M22759-43-22-9	Single AWG 22 (paired with another single in the bundle)	7.0955 9.0067	3.5631 12.1593	1.7769 14.1011	0.8888 14.9201

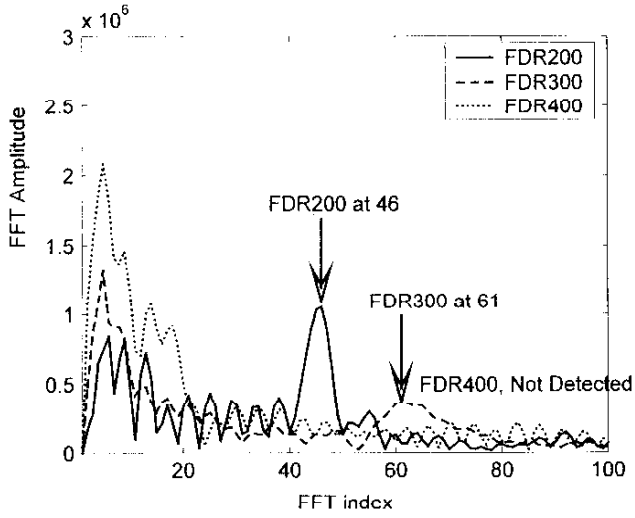

Fig. 11. 1024 points FFT response of a 361-in-long 4-shielded cable by the PD-FDR200 (100–220 MHz), PD-FDR300 (150–300 MHz), and PD-FDR400 (180–400 MHz).

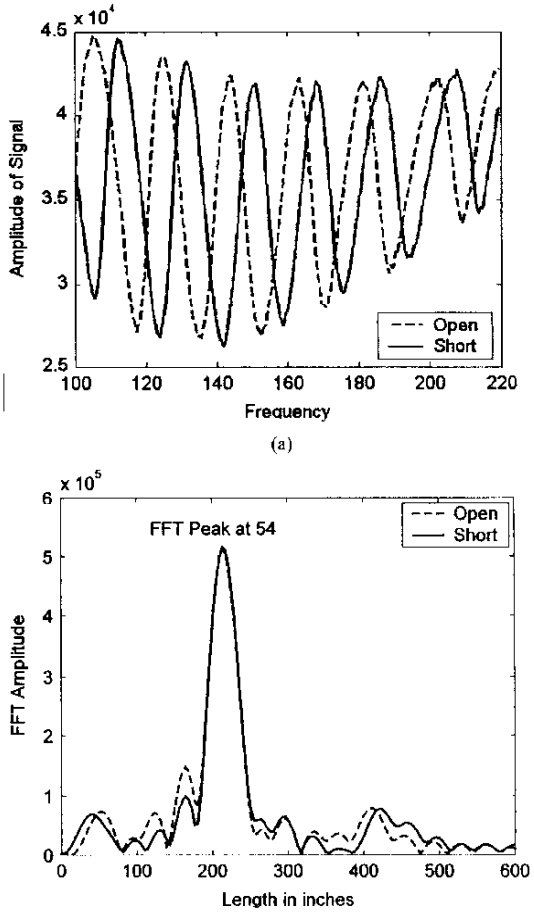

Fig. 12. (a) Open and short responses of 214-in shielded quad wire (Item 9 in Table I) for PD FDR 200. (b) 2048 point FFT of open and short responses of 214 in shielded quadruple wire. The estimated length is 213.8 in.

wire. Thus, the load (open or short) cannot be predicted unless a baseline for the specific type of wire under test is available to give an empirical measurement of the expected phase of either an open or a short. Partial open or short circuits (assuming they were large enough to produce a significant reflection) would further complicate this measurement, so in practice the PD-FDR method appears to be unreliable for practical determination of the type of fault on the end of the wire.

V. CONCLUSION

While this paper demonstrates the accuracy and design trade-offs for the PD-FDR unit on a single wiring harness, it is also important to recognize the limitations of this method and areas where further progress is needed. First, all of the wires in this bundle were tested with a second wire in the bundle as the return path for current, and this is typically available for a majority of aircraft wires. For a minority of wires, for example those that go

to individual sensors distributed throughout the plane, a pair of wires may not be available, and the aircraft ground may need to be used as the return path for current. We have yet to be able to demonstrate consistent and accurate results for PD-FDR with single wires that have no other wire available to use as a return path for current. A capacitance sensor [20] or spread spectrum reflectometer [11] could be used instead. Second, the effect of wires that are spliced into "tree-shaped" networks has not been considered in this paper. For such a case, the PD-FDR returns multiple reflection locations, each corresponding to a junction or termination, and these need to be analyzed in tandem to map out the network. [17]. Third, with some modification, the PD-FDR might be used for low frequency live signals (less than 100 kHz) [21], but it is not optimal for this application, and cannot be used on lines carrying high frequency data signals. When tested on 28-V dc lines, the measurements were within 1 in of those reported in this paper, but it is not clear if the approximately 1-mV signal from the FDR would interfere with the voltage line. The spread spectrum methods are better suited for live wire applications [11]. With proper consideration of these issues, the PD-FDR shows excellent promise as a fault location modality for realistic aircraft harnesses. Finally, this like other reflectometry methods, relies on receiving a significant amount of reflected power from the discontinuity being tested, so is only suitable for "hard faults" such as open and short circuits and not for small anomalies like frays or chafes in the wire.

REFERENCES

[1] C. Furse and R. Haupt, "Down to the wire: The hidden hazard of aging aircraft wiring," *IEEE Spectr.*, pp. 35–39, Feb. 2001.

[2] "Wiring Integrity Research (WIRE) Pilot Study A0SP-001-XB1,", Aug. 2000. NASA.

[3] "Review of Federal Programs for Wire System Safety,", Nov. 2000. NSTC, *White House Report*.

[4] N. A. Mackay and S. R. Penstone, "High-sensitivity narrow-band time-domain reflectometer," *IEEE Trans. Instrum. Meas.*, vol. 23, no. 2, pp. 155–158, Jun. 1974.

[5] C. S. Chen, L. E. Roemer, and R. S. Grumbach, "Cable diagnostics for power cables," in *IEEE Annu. Conf. Electrical Engineering Problems in Rubber and Plastic Industries*, Apr. 1978, pp. 20–22.

[6] B. Waddoups, "Analysis of reflectometry for detection of chafed aircraft wiring insulation," M.S. thesis, Dept. Elect. Comp. Eng., Utah State Univ., Logan, UT, 2001.

[7] M. Schmidt, "Use of TDR for cable testing," M.S. thesis, Dept. Elect. Comp. Eng., Utah State Univ., Logan, UT, 2002.

[8] A. Jani, "Location of small frays using TDR," M.S. thesis, Dept. Elect. Comp. Eng., Utah State Univ., Logan, UT, 2003.

[9] K. Jones *et al.*, "Adapative apparatus for transmission line analysis," U.S. Patent 20 020 169 585, Mar. 11, 2002.

[10] V. Taylor and M. Faulkner, "Line monitoring and fault location using spread spectrum on power line carrier," in *IEE Proc. Generation Transmission and Distribution*, vol. 143, Sep. 1996, pp. 427–434.

[11] C. Furse, P. Smith, and M. Safavi, "Feasibility of spread spectrum reflectometry for location of arcs on live wires," *IEEE J. Sens.*, to be published.

[12] C. Furse and N. Kamdar, "An inexpensive distance measuring system for navigation of robotic vehicle," *Microw. Opt. Technol. Lett.*, vol. 33, no. 2, pp. 84–97, Apr. 2002.

[13] P. J. Medelius and H. J. Simson, "Non-Intrusive impedance-based cable tester," U.S. Patent 5 977 773, Nov. 2, 1999.

[14] R. J. Woodward, "Using frequency domain reflectometry for water level measurement," M.S. thesis, Utah State Univ., Logan, 2000.

[15] D. A. Noon and M. E. Bialkowski, "An inexpensive microwave distance measuring system," *Microw. Opt. Technol. Lett.*, vol. 6, pp. 287–292, Apr. 1993.

[16] N. Kamdar, "Application of distance measuring system for location of robotic vehicles," M.S. thesis, Dept. Elect. Comp. Eng., Utah State Univ., Logan, UT, 1998.

[17] A. Jayakar, "Use of FDR for analysis of cable trees," M.S. thesis, Utah State Univ., Logan, UT, 2000.

[18] *TDR100 Instruction Manual* [Online]. Available: ftp://ftp.campbellsci.com/pub/outgoing/manuals/tdr100.pdf

[19] C. Furse, Y. C. Chung, R. Dangol, M. Nielsen, G. Mabey, and R. Woodward, "Frequency domain reflectometry for on board testing of aging aircraft wiring," *IEEE Trans. Electromagn. Compat.*, vol. 45, no. 2, pp. 306–315, May 2003.

[20] J. Pruitt, "Simulation and analysis of four navy aircraft wiring harnesses using frequency domain reflectometry," M.S. thesis, Utah State Univ., Logan, UT, 2002.

[21] K. Konda, "Hardware connectivity methods for live wires," M.S. Thesis, Dept. Elect. Comp. Eng., Utah State Univ., Logan, UT, 2003.

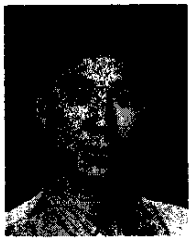

You Chung Chung (S'94–M'00–SM'04) received the B.S. degree in electrical engineering from Inha University, Inchon, Korea, in 1990, and the M.S.E.E. and Ph.D. degrees from University of Nevada, Reno (UNR), in 1994 and 1999, respectively.

Currently, he is with Daegu University, Kyungbuk, Korea. He was a Research Assistant Professor of electrical and computer engineering at University of Utah, Salt Lake City and Utah State University, Logan. He has worked in the Center of Excellence for Smart Sensors and CSOIS, Utah State University. His research interests include computational electromagnetics, optimized antenna and array design, conformal and fractal antennas, smart wireless sensors, aging aircraft wire detection sensors, optimization techniques, EM design automation tool development, and genetic algorithm.

In 1996, Dr. Chung received an Outstanding Teaching Assistant Award from UNR. He also received an Outstanding Graduate Student Award in 1999. The National Science Foundation sponsored his 1999 IEEE TRANSACTIONS ON ANTENNAS AND PROPAGATION paper presentation. In 2000, he received the Third Student Paper Award from URSI International Student Paper Competition.

Cynthia Furse (M'84–SM'99) is the Director of the Center of Excellence for Smart Sensors at the University of Utah, Salt Lake City, Associate Professor in the Electrical and Computer Engineering Department, and Research Lead with LiveWire Test Laboratories, Inc., Salt Lake City, UT. The Center focuses on imbedded sensors in complex environments, particularly sensors for anomalies in the human body and aging aircraft wiring. She has directed the Utah "Smart Wiring" program since 1997. She teaches electromagnetics, wireless communication, computational electromagnetics, microwave engineering, and antenna design.

Dr. Furse was the Professor of the Year in the College of Engineering at Utah State University in 2000, Faculty Employee of the Year 2002, a National Science Foundation Computational and Information Sciences and Engineering Graduate Fellow, IEEE Microwave Theory and Techniques Society Graduate Fellow, and President's Scholar at the University of Utah. She is the chair of the IEEE Antennas and Propagation Society Education Committee, and Associate Editor of the IEEE TRANSACTIONS ON ANTENNAS AND PROPAGATION.

Jeremy Pruitt (S'99–M'03) received the B.S. and M.S. degrees in electrical engineering from Utah State University, Logan, in 2002 and 2003, respectively.

While at Utah State University, he worked as a Teaching Assistant a Research Assistant and interned with the Naval Air Command Patuxent River Naval Base. His research and internship focused on wiring diagnostics and fault detection. He currently works for the Signal Exploitation and Geolocation Division, Southwest Research Institute. His professional interests include antennas, electromagnetics, RF, microwave, and analog circuit design.